Hydrodynamic Performance Evaluation of an Ellipsoidal Nose for a High Speed under Water Vehicle

K. N. S.Suman [a], D. Nageswara Rao [a], H. N. Das [b], G.Bhanu Kiran [c,*]

[a] *Department of Mechanical Engineering, Andhra University, Visakhapatnam-530 003, India*

[b] *Hydrodynamics Research Wing, Naval Science and Technological Lab, Visakhapatnam - 530 027, India*

[c] *Department of Mechanical Engineering,GITAM University,Visakhapatnam-530 045 India*

Abstract

The present work attempts to evaluate the functionality of an ellipsoidal head designed and fabricated for improved hydrodynamic performance of a high speed under water vehicle, which is predominantly used in defense applications. The importance of proper geometric shape for head portion of an under water vehicle is studied by the performance evaluation of different profiles through computational analysis. It is identified that the hydrodynamic performance of the vehicle can be improved with head having ellipsoidal profile. The designed vehicle having ellipsoidal heads of different major to minor axes ratio is fabricated and tested experimentally to validate the computational results.

Keywords: Under Water Vehicle; Drag; Cavitation; Hydrodynamic Performance; Design.

1. Introduction

High speed under water vehicles like torpedoes, submersibles, submarines are increasingly being proposed for diverse defence and commercial applications. These under water vehicles intended to design for better hydrodynamic and structural performance require cavitation susceptibility, minimum hydrodynamic resistance (drag) and structural weight for increasing payload carrying capacity, speed and operating range. The design of a vehicle with the above mentioned goal is always been of considerable interest to the designers of marine hydrodynamic structures.

Research in the area of design of under water vehicles has been carried by many researchers, in which Lumley [1] considered that the techniques to improve the hydrodynamic performance i.e. minimization of drag, regulating the dynamic pressure distribution etc., of a vehicle broadly can be classified as conventional and non-conventional. According to him the techniques involving stabilization of the boundary layer are referred as conventional techniques. Prandtl [2] used two methods of boundary layer control, which are suction and movement of the surface in the direction of flow. Schlichting[3] reported that

appropriate hull shape is a known means for extending the laminar boundary layer flow to a greater length. Several authors found that transition from laminar to turbulent flow can also be delayed by the use of suitable hull shaping. Methods for laminar and turbulent boundary layer flows with suction applied to prevent separation are discussed by Wuest [4]. The purpose of removing the fluid from boundary layer through suction is to stabilize the laminar layer and prevent it from becoming turbulent. Mecormick [5] was able to do some experimental investigation on these suction slots based on the findings of Loftin and Burrows [6]. Change of viscosity of the fluid can be considered as a non-conventional technique which is attempted by Toms[7]. Hoyt and Fabula [8], Thruston and Jones [9] performed experiments to predict the polymer concentration for maximum effectiveness in changing the viscosity of the fluid. M.Zahid Bashir, S.Bilal & M.A.Khan [11] numerically and experimentally determined the cavitation inception number for three axisymmetric head forms, at zero degree angle of incidence and compared with CFD results. John Lindsley Freudenthal [12] performed water tunnel experiment for the prediction of drag over a prototype model of axisymmetric submarine hull, compared the experimental results with CFD results. He also evaluated the formula for drag coefficient that uses only mean velocity measurements of axisymmetric body using assumptions of a self-similar wake and power law behavior of the wake scales. Paster, D. Raytheon Co., Portsmouth [13] explained how a reasonable hydrodynamic design can result in low drag and noise with minimum compromise in volume, which inturn results for reduced development and production costs. They suggested methods for estimating the drag as a function of speed, shape and size. Lt Cdr A Saiju and Cmde N Banerjee [14] performed wind tunnel

---

* Corresponding author. e-mail:bk_1381@yahoo.co.in

experiment for nose cone optimization of an underwater vehicle. They compared the results of wind tunnel over cavitation tunnel experimental results. C. J. Lu, Y. S. He, X. Chen, Y. Chen [15] focused on systematic study of Steady and unsteady flows of natural and ventilated cavitation through experimental observation. Some significant problems concerning ventilated cavitating flows, such as the critical status, hysteresis, surface wave, wall effect and ventilation manner, were investigated.

Review of the work reported so far reveals that several direct and indirect techniques were proposed separately by many researchers for improving the hydrodynamic performance of the vehicle. But many of these techniques demand for excessive experimentation which involves high cost and are mainly dependent on the unreliable fluid conditions prevailing during the motion of the vehicle in sea water. Of all the methods reported so far for better

vehicle performance, hull shaping with a proper profile costs minimum and thus attracting the researchers to investigate on these lines. The parameters of the hull profile such as height, thickness and radius have a considerable effect on the performance of the vehicle with regard to its hydrodynamic characteristics.

The objective of the present paper is to design a better hull shape which is one of the popular techniques available to the designers for serving the dual purpose aim of drag reduction and pressure regulation for the proposed vehicle. An investigation based on numerical and experimental results is illustrated with reference to a specific model of an under water vehicle. Numerical analysis using the concept of Computational Fluid Dynamics (CFD) was firstly done to compute the hydrodynamic parameters such as pressure distribution, drag of the vehicle. The numerical predictions are compared with experimental investigations performed in wind tunnel.

2. Problem Description

The profile of an under water vehicle considered is shown in Fig.1. The hull body of the vehicle has three portions namely (a) nose cone or head (b) cylindrical middle compartment and (c) tail. Out of these three

portions head is an important portion from pressure point of view, which may lead to cavitation. Cavitation susceptibility of the hull, apart from the drag is a challenging criterion for the designers.
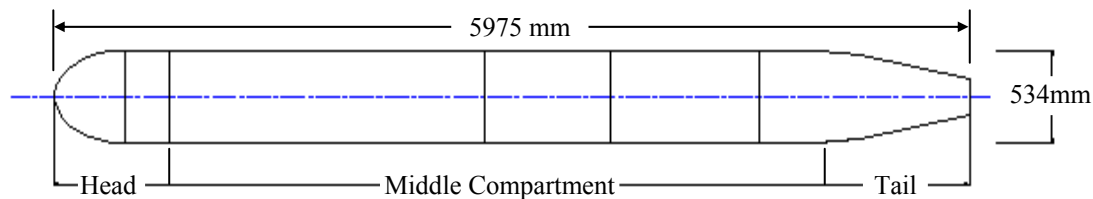

Figure 1: Profile of the under water vehicle

Head cavitation of these vehicles especially detrimental for effective functioning of its own sonar performance. Since cavitation inception is expected to occur at the location of minimum negative pressure, information about the unsteady pressure distribution over the torpedo head while underway is of vital importance to the designer. The location and magnitude of the minimum pressure on the

body are determined for finding out the appropriate locations of the sensors such that their performance is least effected by the onset of cavitation. Apart from this, head portion of the vehicle should have high payload carrying capacity. Hence the design of a proper head profile which can serve as a nose cone of the under water vehicle satisfying all the above mentioned factors is important.

3. The Design Approach

The total length of the vehicle considered is of 5975 mm length and the middle compartment is of 534 mm diameter as shown in Fig.1. Four different axi-

symmetric Head profiles (Fig.2) are considered for analyzing the drag and dynamic pressure distribution over the body.

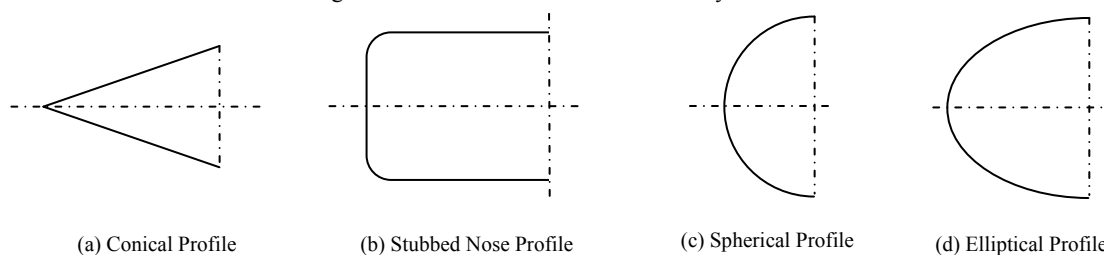(a) Conical Profile   (b) Stubbed Nose Profile   (c) Spherical Profile   (d) Elliptical Profile

Figure 2: Head profiles considered for analysis

All the above Head profiles are selected based on their aerodynamic characteristics available in the literature [10].

As it is decided not to alter the dimensions of the cylindrical middle compartment, head profiles dimensions

are selected in such a way that they can be properly attached to the cylindrical middle compartment which is

having a constant diameter.

Table 1: Dimensions of the Head profiles

Sl. No.	Profile	Dimensions
1	Cone	Height: 420 mm
		Radius: 267 mm
2	Stubbed nose profile	Length: 420 mm
		Radius: 267 mm
		Edge Radius: 5 mm
3	Sphere	Radius: 267 mm
4	Ellipse	Major Axis: 420 mm
		Minor Axis: 267 mm

4. Computational Analysis

The vehicle has an axisymmetric geometry and the bare hull is only taken for the analysis. The present exercise is intended to compute the drag and dynamic pressure distribution over the body in the flow field. The flow is assumed to be steady, incompressible and turbulent in nature. The computations presented in this work use, FLUENT 6.1.18 solver for solving the turbulent flow field over an arbitrary geometry and GAMBIT, the preprocessor of fluent as grid generator.

1.1. Grid Generation

The vehicle is modeled as a 2D axisymmetric body. The flow field boundaries are presented in fig. 3. The gridlines are geometrically stretched close to the body to obtain lesser spacing near the surface of the body than in the far field. A flow domain measuring 36 m × 4 m is considered to accommodate the 5.975 m long body and the grid generated in the entire flow field appears as in fig.4. The grid generated is of H type in nature and quite fine which contains 32,300 cells.
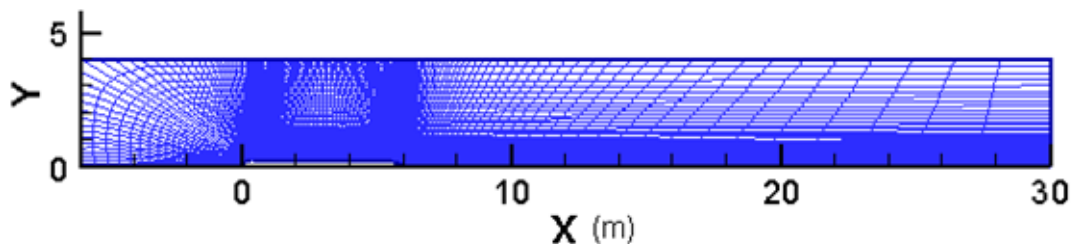

Figure 3: Boundary of the flow domain

4.2 Flow Solver

Fluent 6.1.18 uses a finite volume method for discretization of the flow domain. The Reynolds Time Averaged Navier-Stokes (RANS) equations are framed for each control volume in the discretized form. Pure upwind scheme is used for the momentum flux discretization.

STANDARD scheme is used for pressure and a SIMPLE (Strongly Implicit Pressure Link Equations) procedure is used for calculation of pressure field from the continuity equation.

4.2.1 Turbulence modeling

The eddy viscosity based $k - \varepsilon$ (standard) model is used in the present work where the additional turbulent stresses arising out of the turbulent fluctuations are assumed to be replaced by viscous type stresses analogous to their laminar counterpart. As a result of this eddy

viscosity hypothesis, the viscosity μ in all the transport equations is replaced by $(\mu_l + \mu_t)$ where μ_l is the laminar viscosity and μ_t is the turbulent or eddy viscosity. Unlike μ_l in laminar flows however, the turbulent or eddy viscosity μ_t is not a fluid property but a function of the local state of turbulence defined by the turbulence kinetic energy, k and its dissipation rate ε as follows:

$$\mu_t = \rho C_\mu k^2 / \varepsilon$$

The field distribution of k and ε are evaluated solving the relevant transport equations.

4.2.2 Boundary conditions

The following boundary conditions are used for solving the flow field generated over the body: (i) Inlet velocity, (ii) Outlet pressure, (iii) Symmetry axis and (iv) Rigid walls. At inlet planes the known boundary values are prescribed in terms of velocity, turbulent kinetic energy - **k** and turbulent dissipation energy - **ε**. At the outlet gauge pressure is set to zero so that it remains at operating pressure. The axis of revolution is set as symmetry axes. At the wall all the two velocity components are set to zero.

For turbulent flow, the field values of k and ε are prescribed at the inflow boundaries. But the turbulence scalar equations are usually source dominant and the results therefore are more or less insensitive to the inlet field values prescribed. However, if the eddy viscosity level at the inlet is too low, numerical problems may arise. Assuming that the equations are valid only for fully turbulent flow, the inlet values of turbulent kinetic energy (k) is chosen as $10^{-4} * U^2$ and values of ε are so chosen that the inlet eddy viscosity is of the order of five times the laminar viscosity.

5.   Computational Results and Discussions

Computations are performed for the flow velocity between 5 to 6 m/s satisfying the turbulent flow conditions. Control volumes are generated over the entire full-length model of the torpedo.   But the pressure distribution is taken only on the head portion and extending to some part of middle portion, without giving importance to the later part of the body. The pressure distribution curves obtained for all the four different hull geometries are shown in figs. 5a-5d.   The values of minimum negative pressure co-efficient (Cp) obtained from pressure distribution graphs and drag coefficient (CD) for all the hull geometries are presented in the Tables 2 and 3 respectively.

Table 2: Values of minimum pressure co-efficient for different profiles

Profile	Minimum Pressure Co-efficient (Cp)
Cone	-1.72
Stubbed nose profile	-0.98
Sphere	-0.721
Ellipse	-0.443

Table 3: Comparison of drag for different profiles

Profile	Form Drag	Skin Friction Drag	Overall Drag
Cone	0.13901508	0.0867318	0.22574688
Stubbed nose profile	0.12013323	0.089248875	0.2093821
Sphere	0.068183163	0.10391882	0.17210198
Ellipse	0.05470272	0.10500373	0.15970645

645

(a) conical profile

(b) stubbed nose profile
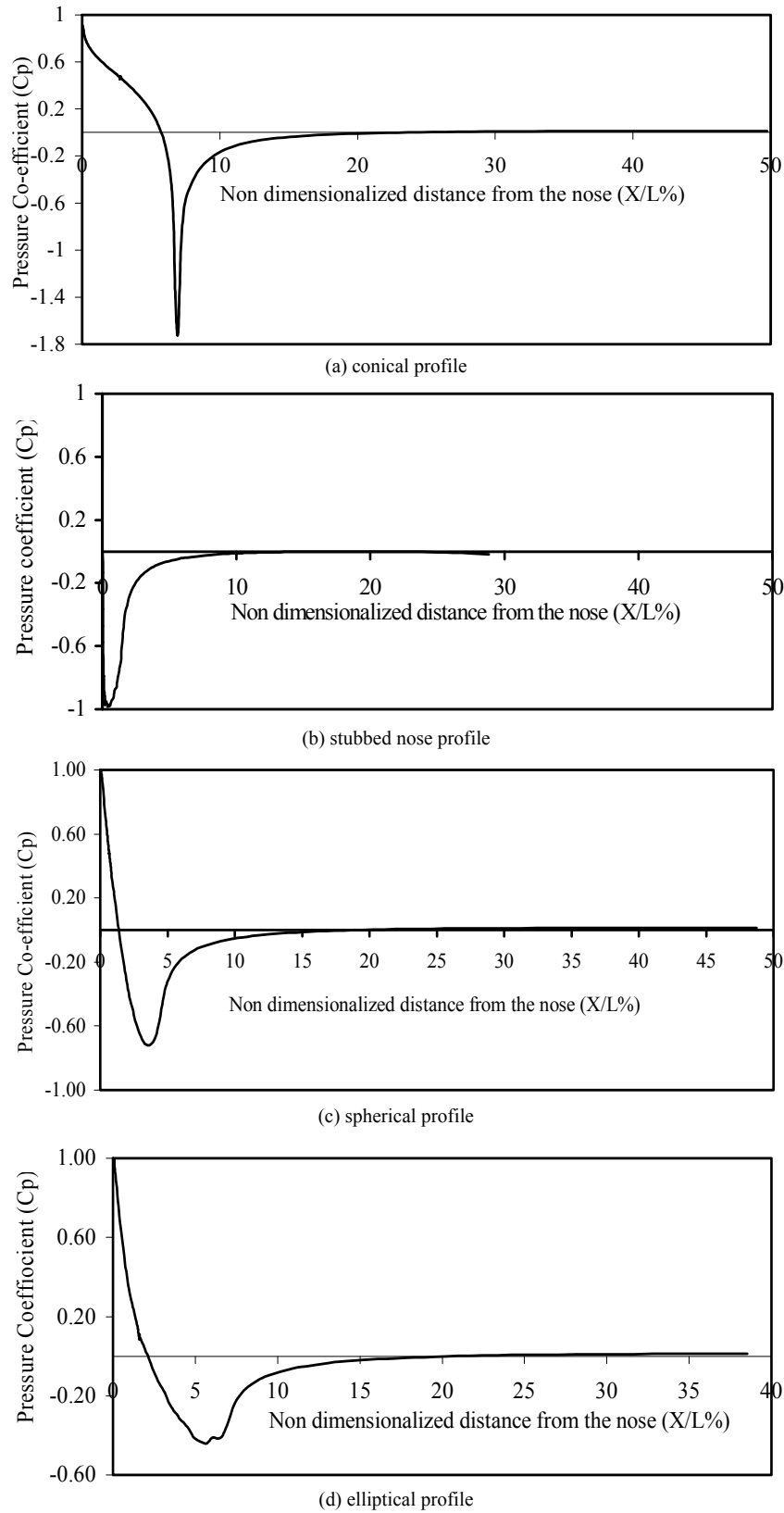
(c) spherical profile

(d) elliptical profile

Figure. 5: Computational pressure distribution over the vehicle for different head profiles

From the preliminary computational analysis exercised over the hull profile having different head geometries it may be concluded that ellipsoidal head profile is suitable for imparting better hydrodynamic performance to the vehicle. It is further resolved to evaluate the suitable dimensions of the ellipsoidal profile for enhancing the

performance of the vehicle in terms of hydrodynamic aspects. The minor axis length is kept constant since it is considered not to alter the radius of the cylindrical middle compartment. By varying only the major axis length of the ellipsoidal head, various profiles are generated. These ellipsoidal profiles having different major to minor axis ratios were solved again for evaluating their hydrodynamic performance and extracting suitable dimensions.

6.   Experimental Investigations

The hydrodynamic characteristics are evaluated computationally for the ellipsoidal heads of different ratios of major to minor axes. These results are validated through experimentation carried out in a low speed wind tunnel on the fabricated ellipsoidal heads. The tunnel is of open circuit type where the air is drawn from the atmosphere and passes through the test section before it is discharged at reduced velocity back into atmosphere. The test section free stream Mach number is kept well below 0.3 and the facility can be extended to predict and validate the fluid dynamic characteristics of a body exposed to a flow in one medium to the flow in different medium. The various compartments in the wind tunnel and their specifications are presented in table 4.

Table 4: Wind tunnel compartments and specifications

Sl.No.	Compartment	Dimensions
1	Test Section	2 × 2 × 4.0 m
2	Plenum Chamber	4.3 × 4.3 × 4.0 m
3	Contraction	Section varying from 4.3 m × 4.3 m to 2 m × 2 m, 4.0 m long
4	Diffuser	Section varying from 2 m × 2 m to 3.048 m diameter of circle, 7.8 m long
5	DC motor	125 KW at 750 rpm
6	Fan	Sweep diameter 3.04 m, 12 blades made of CFRP
7	Maximum wind speed at test section	60 m/sec

A 125KW DC variable speed motor drives the 12 blades CFRP tunnel fan for achieving the desired wind speed in the tunnel test section. Pitot tube positioned in the plenum chamber 275mm above the base at the centerline of the tunnel measures the total pressure head. The free stream pressure at different locations in the tunnel is obtained by a system of Pitot tubes arranged at these locations flushed with the surface of the tunnel.

7. Pressure Tapping and Instrumentation on The Fabricated Models

Three ellipsoidal heads having different major to minor axis ratios are fabricated with Fiber Reinforced Plastic (FRP) upto a thickness of 6-8mm and prepared for experimentation. These heads are attached separately to a smooth cylindrical body resembling the middle portion of the vehicle modeled during computational analysis. Thus the fabricated full scale model without tail portion resulted in a blockage of approximately 4% which is considered to be acceptable. The model gave Reynolds number large enough to ensure that the it is essentially operated in the fully turbulent regime.

7.1 Pressure Tapping

Pressure taps of 1.4 mm diameter are drilled along vertical centerline on the surface of the model fabricated. Of, these 6 pressure taps are symmetrically distributed at bottom half of the model to verify yaw and pitch. 1.9 mm SS tubes of 1 mm inner diameter are inserted in to the pressure taps on the model from inside so as to make it flushed with the outer surface of the model (Fig.6).

Figure 6: Drilling of pressure holes on the model

7.2 Instrumentation

Two scanivalves (low pressure transducers) having 48 selectable ports are mounted inside the model. These scanivalve ports are connected to the SS tubes press fitted to the pressure tapping on the body by means of 1.4 mm urethane tubes. Each scanivalve's signal output, control

input and port address output connections are brought down to the instrumentation room and connected to the signal conditioner, solenoid controller and decoder respectively. The signal conditioner out put voltages are acquired by a Data Acquisition System (DAS) (Figs.7 and 8).
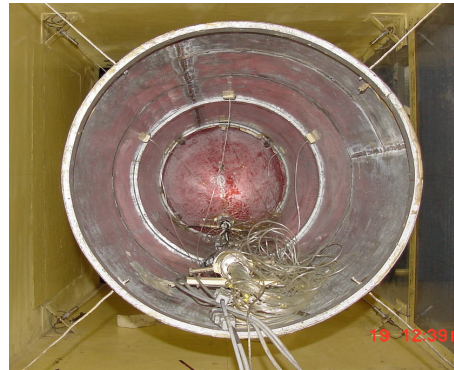

Figure 7: Pressure tapping and scanivalve arrangement

Figure 8: Pressure tapping instrumentation over the entire model

8. Mounting of The Model and Test Method

The model consisting of fabricated ellipsoidal head and cylindrical body is mounted along the centre line of the test section by suspending it from eight 3 mm wire ropes at 2 locations along the length. The model is accurately aligned along the centerline of the tunnel using spirit level and measuring distance from sidewalls precisely (Fig.9). Fan drive system is operated at different RPMs to achieve variable wind speeds in order to subject the model to a fluid flow having different Reynolds numbers. Pressure distribution at various Reynolds numbers are obtained from the scanivalves and are recorded on-line. The

recorded data of pressures are plotted in terms of pressure co-efficient (C_p) vs the distance from the nose portion.

9. Discussion of Results

Investigations are carried out on the basic head profiles such as conical, stubbed nose, spherical and ellipsoidal profiles to arrive at the better profile for the under water vehicle of standard dimensions. It is concluded that ellipsoidal profile is the better among all the profiles for providing good hydrodynamic characteristics to the vehicle. It is further considered to alter the major to minor axes ratio of the ellipse and analyze the hydrodynamic performance of the vehicle to investigate the suitable dimensions of the ellipse.

Front View

Rear View

Figure 9: Ellipsoidal Model of 2.3:1 major to minor axes ratio mounted in the test section

9.1 Analysis of Computational Results for Minimum Pressure Value and Cavitation Susceptibility of the Vehicle

Cavitation is normally expected to occur at the location of minimum pressure occurrence. The value of the minimum pressure gives the measure of velocity and depth at which the vehicle should be operated without any cavitation. The location of the minimum pressure occurrence also gives the measure of placement of sensors in the head, so that their performance is least effected by the onset of cavitation. The information about the magnitude and location of the minimum pressure co-efficient for different heads of the vehicle are presented in Table 5. The operating velocity range or cavitation speed of the vehicle is calculated from the tabulated results as:

$$Cp = \frac{P - P_{ref}}{0.5 \rho V^2}$$ at different depths of operation.

Where Cp = Pressure Co-efficient , P = Actual pressure acting at location of interest, P_{ref} = atmospheric pressure + $\rho g h$ ρ = density of fluid, kg/m^3

g = acceleration due to gravity, m/sec^2 , h = Vehicle operating depth, m

V = velocity of the vehicle, m/sec

Table 5: Comparison of minimum pressure co-efficient for different Ellipsoidal Heads

Axes ratio of Ellipsoidal Heads	Value of Minimum Pressure Co-efficient	Location of occurrence (X/L%)
1.6:1	-0.443	5.6
1.95:1	-0.309	6.68
2.32:1	-0.246	7.59
2.7:1	-0.198	8.52
3:1	-0.163	9.32
4:1	-0.106	12.11
5:1	-0.0719	14.37

From these results, it is observed that the pressure co-efficient is getting decreased with the increase in dimensions of the head profile. It is also observed that the location of the negative pressure co-efficient is tending to shift away from the nose portion as the axes ration increases (major axis).

Table 6: Cavitation inception speed for various ellipsoidal heads at different depths of operation

Head (axes ratio)	Cavitation inception speed in m/sec at the operation depth of			
	10 m	12 m	30 m	40 m
1.6:1	29.69	36.39	42.04	47.01
1.95:1	35.55	43.58	50.34	56.30
2.32:1	39.84	48.85	56.43	63.11
2.7:1	44.41	54.46	62.90	70.35
3:1	48.95	60.01	69.32	77.52
4:1	60.70	74.62	86.20	96.40
5:1	73.70	90.40	104.42	116.77

It may be observed from the table 6 that with the increase of the major axis, the operating velocity range of the vehicle increases at all depths. The operating velocity of the vehicle can be selected as per the nose shape or vice-versa to avoid cavitation.

9.2 Analysis of Drag

A graphical depiction of variation of overall drag, form drag and viscous drag for the vehicles with different ellipsoidal heads is in fig.10. It can be observed from the results that due to increase in length of the ellipsoidal head there is decrement in overall drag of the vehicle which composes of form drag and viscous drag. The viscous drag remains constant, as this is due to the body portion of the vehicle, which is parallel to the flow. In the present case the cylindrical portion of the body is parallel to the flow and its dimensions are kept constant. Hence the viscous drag remains constant.
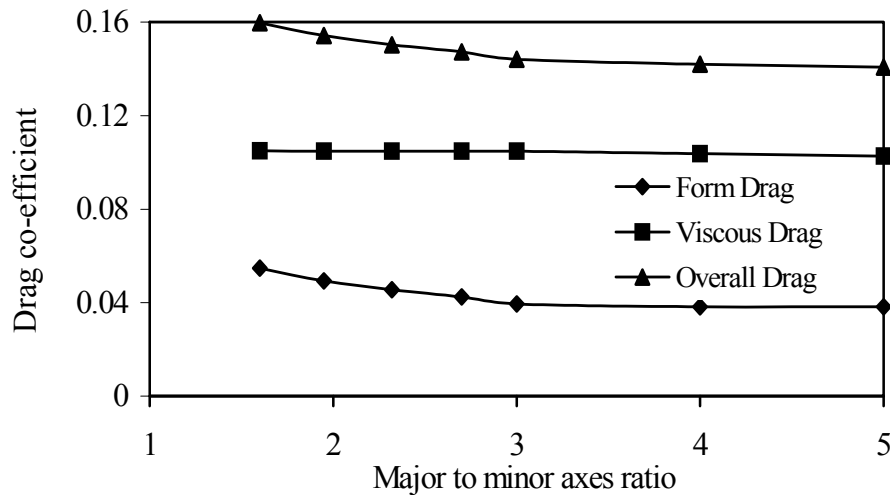
Figure10: Variation of drag co-efficient for different axes ratios of ellipsoidal profiles

The form drag obtained for different profiles is decreasing as the ratio of major to minor axes of the profile increases. The increase in momentum transfer within the boundary layer due to the increase in the axes ratio of the profile is one of the reasons for decrease in pressure drag.

The notable feature which can be observed from the above results is that the variation of form drag of the vehicle has become almost constant beyond the axes ration value of 3. The stabilization of the boundary layer beyond an axes ratio of 3 may be one possible reason for the negligible change in form drag. It is also observed from the results of pressure distribution and cavitation analysis that the vehicle consisting of ellipsoidal head with major to minor axis ratio of 3 is less susceptible to cavitation in the operating range. Hence it can be concluded that ellipsoidal head with major to minor axis ratio of 3 is sufficient for providing good hydrodynamic characteristics to the present under water vehicle.

9.3 Validation

The validity of the numerical analysis carried on different ellipsoidal heads practically tested on the fabricated noses using palm fibre reinforced plastic. Apart from the elliptical profile with an axes ratio of 3 arrived through numerical analysis another two ellipsoidal noses having major to minor axes ratio as 1.6, 2.32 are fabricated to verify the validity of the numerical results.

The experiments are carried on models developed in a wind tunnel at different wind speeds ranging from 14 m/sec to 60 m/sec. Error analysis for the experimental results is performed to estimate degree of uncertainty associated with the experimental results. Degree of Uncertainty associated with experimentally found pressure coefficient along the length of the vehicle for different ellipsoidal heads is given in Fig 11.

The pressure distribution plots practically obtained for all the bodies having different ellipsoidal heads are compared with corresponding computational results (Figs.12-14) and Table 7. The results obtained have shown a small deviation between fabricated and computed values. It may be observed that the trend of the pressure distribution plotted from experimental values is in close agreement with that of computational values. In the computational analysis the pressure values can be evaluated at many (infinite) locations of the hull and hence a large data can be generated and this enables the plot of the pressure distribution to follow a smooth trend. The experimental set up has limitations in providing pressure tappings over the surface which leads to less data compared to computational analysis and hence deviations in the results are observed. During the computational analysis the hull surface is assumed to be perfectly smooth. In the present model, the surface is made up of hand lay-up technique using coarse fibre which does not yield smooth surface. This also might be one of the reasons for small deviations to occur on the pressure distribution profiles.
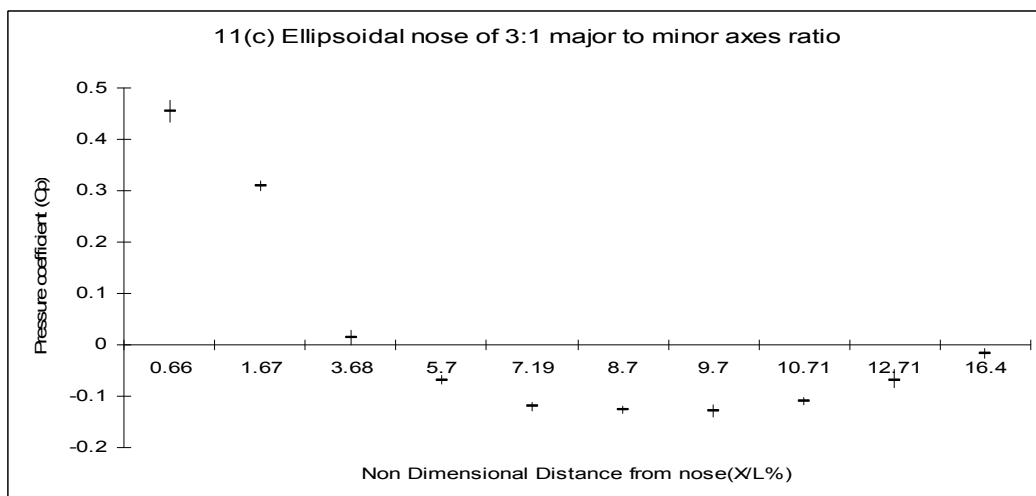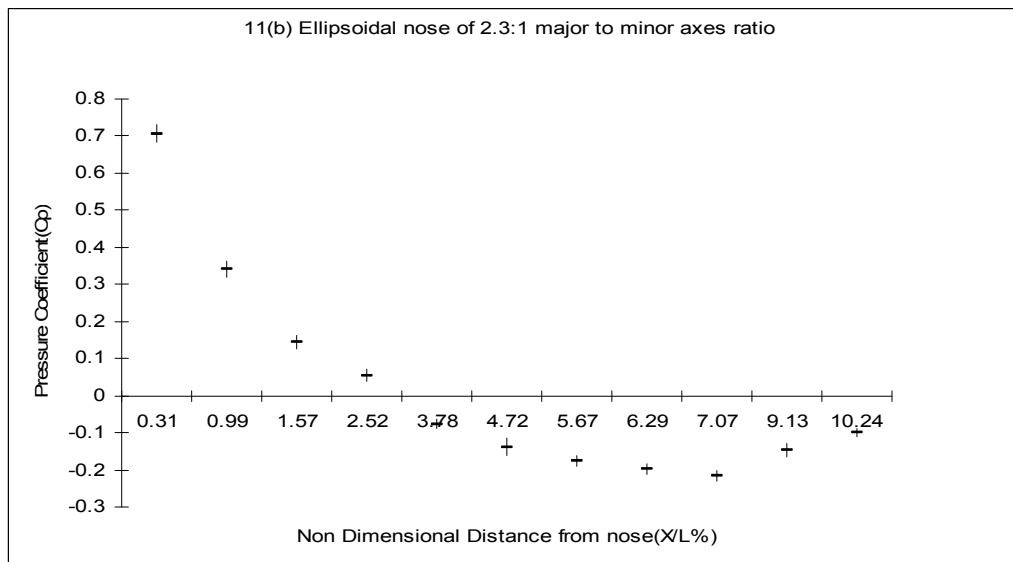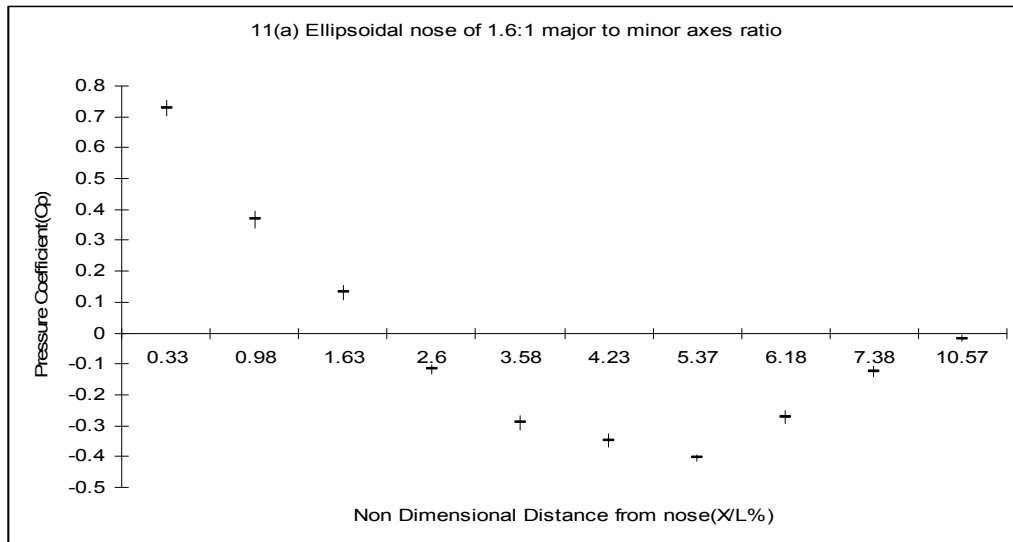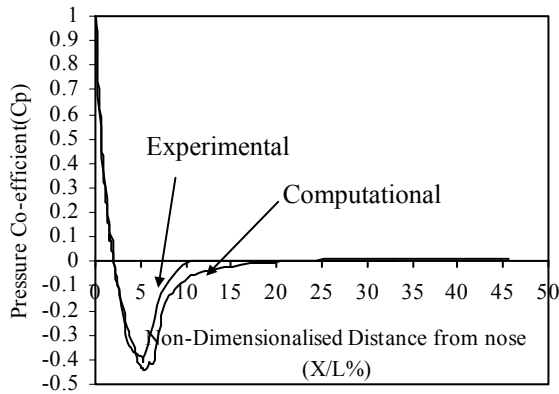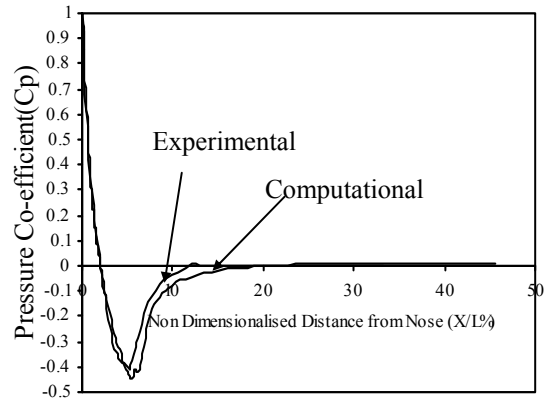
Figure 11: Degree of Uncertainty associated with pressure coefficient along the length of the vehicle for different ellipsoidal heads
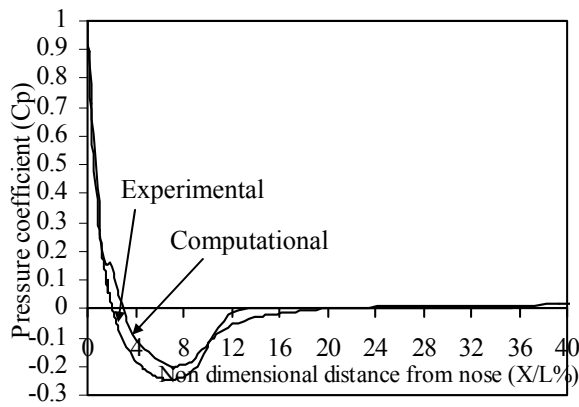
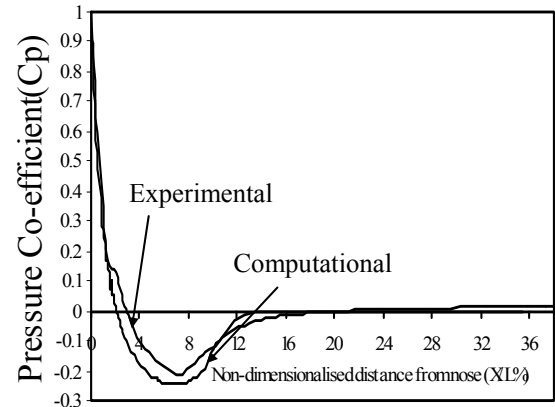(a) Wind speed 25.17 m/s (Reynolds Number 3.36E06)

(b) Wind speed 35.68 m/s (Reynolds Number 4.76E06)

Figure 11: Comparison of pressure distribution obtained over ellipsoidal nose of 1.6:1 major to minor axes ratio for different wind speeds
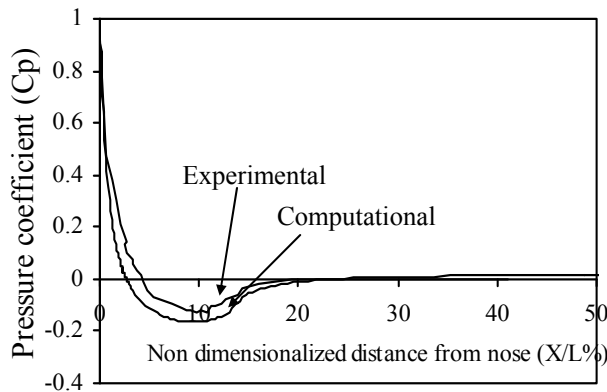

(a) Wind speed 26.8 m/s (Reynolds Number 4.26E06)

(b) Wind speed 35.68 m/s (Reynolds Number 4.76E06)

Figure 12: Comparison of pressure distribution obtained over ellipsoidal nose of 2.3:1 major to minor axes ratio for different wind speeds

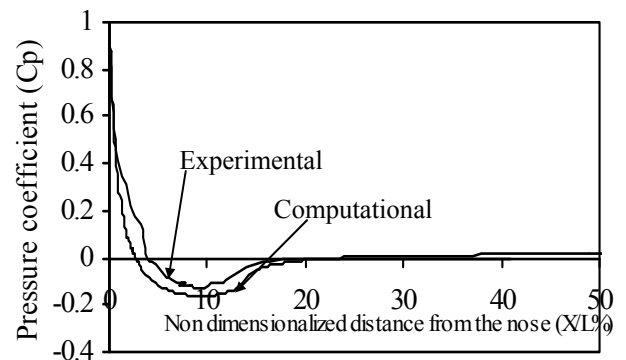(a) Wind speed 26.8 m/s (Reynolds Number 4.26E06)

(b) Wind speed 23.6 m/s (Reynolds Number 3.76E06)

Figure 13: Comparison of pressure distribution obtained over ellipsoidal nose of 3:1 major to minor axes ratio for different wind speeds

Table 7: Comparison of the magnitude and location of minimum pressure co-efficient from experimental and computation analysis

Profile (major to minor axis ratio)	Min. pressure co-efficient	Location of the pressure co-efficient (% of body length)
1.6:1		
Computational	-0.443	5.637
Experimental	-0.404 ± 0.011	5.365
2.32:1		
Computational	-0.246	7.590
Experimental	-0.215 ± 0.014	7.086
3:1		
Computational	−0.1633	9.32
Experimental	−0.1278 ±0.121	9.70

10. Conclusions

The importance of ellipsoidal head for improving the hydrodynamic performance of a high speed under water vehicle having cylindrical mid-section and tapered after body has been identified through computational and experimental analysis. Among the several axi-symmetric head profiles tested

through computational analysis for their hydrodynamic performance, ellipsoidal head resulted to be better nose profile for improving the cavitation susceptibility and minimizing the overall drag of the vehicle. The obtained computational results have been validated by the experimental investigations carried on the full scale model of the vehicle through wind tunnel tests. The results obtained are in close agreement with only minor deviations.

References

[1] Lumley. J.L "Reduction of skin friction drag", Proceedings of 5th Symposium, Naval Hydrodynamics, Norway,1964

[2] Prandtl, "Boundary layer theory, Fluid Motion at Low Viscosity", Verhandlungen International Math. Congress, Heidelberg, 1904

[3] Schlichting, H. Boundary Layer Theory, Mc-Graw Hill Publications,1960

[4] Wuest, W. Theory of boundary layer suction to prevent separation. In: Lachmann G.V. Boundary layer and flow control, Pergaman Press, 196, 196.

[5] McCormick, B.W. "An experimental study of the drag reduction by suction through circumferential slots   on a buoyant propelled axisymmetric body", Proceedings. of 5th Symposium Naval Hydrodynamics, Norway, 1964.

[6] Loftin, J.K. & Burrows, D.L. "Investigations relating to the extension of laminar flow by means of boundary layer suction through slot", NACA report , 1961.

[7] Toms, B.A.. "Some observations on the flow of linear polymer solution through straight tubes at average Reynolds number"', Proceedings of the International Rheological congress, Scheveningen, Holland, vol II, 1948.

[8] Hoyt, I.W. and Fabula, A.G. Effect of additives on fluid friction, In: Freiner (Ed.).Under Water Missile Propulsion, Compass Publication, 1968, 171- 183.

[9] Thruston, S & Jones, R.D. 'Experimental model studies of non-newtonian soluble coatings for drag reduction', In: L.Friener (Ed.). Underwater Missile Propulsion, Compass Publication, 1968, 191-203.

[10] Hoerner, S.F. Fluid Dynamic Drag, Authors Self Publication, New Jersy, 1965.

[11] M.Zahid Basher, S.Bilal & M.A.Khan, "Calculation of flow over Under water bodies with hull and sail", 2nd IBCAST,Burban,Pakistan, 1999.

[12] John Lindsley Freudenthal, "Experimental studies on the dragof an Axisymmetric hull", thesis in aerospace engineering, Mississippi, December 2002.

[13] Paster, D. Raytheon Co., Portsmouth "Importance of Hydrodynamic Considerations for Underwater Vehicle Design" IEEE oceans volume 18, 2003, 1413-1422.

[14] Lt Cdr A Saiju and Cmde N Banerjee, "Cavitation Investigation and nose cone optimization of an under water vehicle using wind tunnel", journal of ship technology, volume 1, 2005, 68-75.

[15] C. J. Lu, Y. S. He, X. Chen, Y. Chen "Numerical and Experimental Research on Cavitating Flows" Proceedings of the Fifth International Conference on Fluid Mechanics, Aug.15-19, 2007, Shanghai, China.